methods

Prediction of PPAR-α ligand-mediated physiological changes using gene expression profiles

Klaus Stensgaard Frederiksen,[1,*] Erik Max Wulff,[†] Per Sauerberg,[§] John Patrick Mogensen,[§] Lone Jeppesen,[§] and Jan Fleckner*

Department of Molecular Genetics,* Novo Nordisk A/S, DK-2880 Bagsværd, Denmark; and Departments of Pharmacological Research 2[†] and Medicinal Chemistry Research III,[§] Novo Nordisk Park, DK-2760 Måløv, Denmark

Abstract **Peroxisome proliferator-activated receptor (PPAR)-α controls the transcription of a variety of genes involved in lipid metabolism and is the target receptor for the hypolipidemic drug class of fibrates. In the present study, the molecular and physiological effects of seven different PPAR-activating drugs have been examined in a rodent model of dyslipidemia. The drugs examined were selected to display varying potencies and efficacies toward PPAR-α. To help elucidate the link between the gene regulation elicited by PPAR-α ligands and the concomitant physiological changes, we have used cDNA microarray analysis to identify smaller gene sets that are predictive of the function of these ligands. A number of genes showed strong correlations to the relative PPAR-α efficacy of the drugs. Furthermore, using multivariate analysis, a strong relationship between the drug-induced triglyceride lowering and the transcriptional profiles of the different drugs could be found.**—Frederiksen, K. S., E. M. Wulff, P. Sauerberg, J. P. Mogensen, L. Jeppesen, and J. Fleckner. **Prediction of PPAR-α ligand-mediated physiological changes using gene expression profiles.** ***J. Lipid Res.*** **2004.** 45: **592–601.**

Supplementary key words dyslipidemia • pharmacodynamics • peroxisome proliferator-activated receptor-α in vivo activation • transcriptional profiling

Peroxisome proliferator-activated receptor (PPAR)-α is recognized as the target receptor for fibrates (1), which are used in the treatment of dyslipidemic patients. Fibrates are recognized to exert their hypolipidemic action by altering lipid metabolism at multiple levels, and PPAR-α is an important regulator of both intracellular and extracellular lipid metabolism. At the intracellular level, PPAR-α regulates a number of genes that encode enzymes involved in the oxidation of fatty acids. These include upregulations of acyl-CoA oxidase (2, 3) the rate-limiting enzyme of peroxisomal β-oxidation, medium-chain acyl-CoA dehydrogenase (4), a central enzyme of mitochondrial β-oxidation, and cytochrome P450 genes (5) involved in microsomal ω-hydroxylation of fatty acids. The induction of fatty acid oxidation, combined with the upregulation of the fatty acid transport protein (6), causes a shift in hepatic fatty acid metabolism with decreased triglyceride synthesis and increased catabolism. These intracellular changes are accompanied by regulation of extracellular lipid metabolism and transport. Induction of the lipoprotein lipase by PPAR-α (7) increases the lipolysis of triglycerides in chylomicrons and VLDL particles. This lipolysis generates precursors to HDL particles. The expression of the two major apolipoproteins of HDL particles, apolipoproteins A-I and A-II, is also upregulated by PPAR-α (8, 9). These events are important factors in fibrate-induced increases of HDL levels. The increased HDL levels may, along with increased cholesterol efflux from peripheral cells through upregulation of the ATP binding cassette transporter A1 transport protein (10), facilitate the reverse cholesterol transport from peripheral tissues back to the liver. Furthermore, apolipoprotein C-III (apoC-III), a major lipoprotein of chylomicrons and VLDL particles, is transcriptionally downregulated by PPAR-α (11).

In the present study, rats fed a high-cholesterol diet (HCD) were used as a dyslipidemic model (12) to study the physiological and transcriptional changes occurring as the result of treatment with various PPAR-α activators. Seven different PPAR-α activators with varying efficacies were selected and tested in the rat model. Using cDNA microarrays, the induced transcriptional changes in the liver were examined. The transcriptional changes of genes encoding apoC-III and peroxisomal enoyl-CoA:hydrotase-

Manuscript received 6 June 2003, in revised form 6 November 2003, and in re-revised form 1 December 2003.

Published, JLR Papers in Press, December 16, 2003.
DOI 10.1194/jlr.M300239-JLR200

Abbreviations: ACBP, acyl-CoA binding protein (diazepam binding inhibitor); apoC-III, apolipoprotein C-III; bifunctional enzyme, peroxisomal enoyl-CoA:hydrotase-3-hydroxyacyl-CoA bifunctional enzyme; Cyp4A10, cytochrome P450 4A10; HCD, high-cholesterol diet; PLS, partial least-squares projection to latent structures; PPAR, peroxisome proliferator-activated receptor.

[1] To whom correspondence should be addressed.
e-mail: ksf@novonordisk.com

3-hydroxyacyl-CoA bifunctional enzyme (bifunctional enzyme) correlated very well to the in vitro-measured PPAR-α efficacies of the drugs. Thus, these genes may be useful as markers for the in vivo efficacy of PPAR-α activators. Furthermore, using multivariate analysis, we identified a set of 19 genes capable of predicting the triglyceride-lowering capacity of each of the drugs.

MATERIALS AND METHODS

DNA microarray analysis

All cDNA inserts were PCR-amplified using the T7 and M13 reverse primers. PCR products (100 μl each) were purified on the Qiagen 96-well PCR purification system and subsequently checked for size and purity on agarose gels. The purified PCR products were mixed 1:1 in DMSO (Sigma, St. Louis, MO) and rearranged in 384-well plates. cDNA targets were spotted in duplicate onto silanized glass slides (Amersham Biosciences, Buckinghamshire, UK) at 55% relative humidity using the Molecular Dynamics Gen. III microarray spotter. All slides were UV cross-linked (50 mJ) in a Stratagene UV cross-linker. Cy-3- and Cy-5-labeled single-stranded cDNA probes were prepared from 15 μg of total RNA from the test and control tissues, respectively. The RNA was incubated with 1 μg of anchored oligo-dT primer at 70°C for 10 min and subsequently chilled on ice for 30 s The primer-annealed RNA was incubated with reaction mixture [1× Superscript II buffer (Life Technologies, Taastrup, Denmark), 10 mM DTT, 200 μM deoxy-guanosine, -adenosine, -thymidine triphosphate, 100 μM dCTP, 100 μM Cy-3/Cy-5-dCTP (Amersham Biosciences), and 200 U of Superscript II reverse transcriptase (Life Technologies)] at 42°C for 2.5 h in a final volume of 20 μl. The RNA template was removed by alkaline denaturation (incubation with 2 μl of 2.5 M NaOH at 37°C for 15 min). Labeled probes were purified on GFX spin columns (Pharmacia Biotech, Uppsala, Sweden). The Cy-3- and Cy-5-labeled cDNAs were mixed 1:1 in hybridization buffer version 2 (Amersham Biosciences) and subsequently 1:1 in formamide (Sigma). The mixed probes were injected into an automated slide processor (Molecular Dynamics, Sunnyvale, CA) and hybridized at 42°C for 16 h. After hybridization, the slide was washed in 1× SSC, 0.2% SDS at 55°C for 10 min and subsequently in 0.1× SSC, 0.2% SDS at 55°C for 10 min. The slide was scanned in a Gen. III microarray laser scanner (Molecular Dynamics). Image analyses were performed with ArrayVision (Imaging Research). All ratios were calculated using background-subtracted, artifact-removed median densities. The Cy-3 and Cy-5 signals were normalized to the spot intensities of all of the spots in each channel.

Northern blots

Total RNA was isolated from tissues using the Trizol reagent according to the instructions of the manufacturer, but with two additional phenol/chloroform extractions. An amount of 20 μg of total RNA was separated on a denaturing gel containing 1% agarose, 20 mM MOPS, 5 mM NaOAc, 6% formaldehyde, and 1 mM EDTA. The size-fractionated RNA was transferred to a Hybond N^+ membrane (Amersham Biosciences) using capillary blotting and was subsequently immobilized by UV cross-linking. cDNA fragments were labeled using the Prime It kit (Stratagene) and [α-^{32}P]dATP (3000 Ci/mmol; Amersham Biosciences). For hybridization and prehybridization, the Express Hyb buffer (Clontech) was used. Signals were detected using a PhosphorImager (Molecular Dynamics) and quantitated with ImageQuant software (Molecular Dynamics).

Quantitative RT-PCR

cDNA was prepared from 1 μg of total RNA from each of the treatment groups using random primers and TaqMan Reverse Transcription reagents (Applied Biosystems, Foster City, CA) according to the manufacturer's instructions. Quantitative PCR was performed on three samples from each treatment group (10-fold dilutions of cDNA) using TaqMan PCR core reagents (Applied Biosystems) on an ABI PRISM® 7000 Sequence Detection System. Primers and 6-carboxyfluorescein-labeled-probes for lipoprotein lipase (LPL), fatty acid transport protein (FATP), acyl-CoA oxidase, and 18S rRNA were ordered as Assays-on-Demand (Applied Biosystems). Probe sequences for these assays were as follows: LPL (ATCCATGGATGGACGGTGACAGGAA; assay Rn00561482_m1), FATP (TGTCAAATATAATTGCACGGTAGTG; assay Rn00585821_m1), acyl-CoA oxidase (TGCTGCAGACAGCCAGGTTCTTGAT; assay Rn00569216_m1), and 18S rRNA (TGGAGGGCAAGTCTGGTGCCAGCAG; assay HS99999901_s1). Data were analyzed using ABI Prism 7000 SDS software (version 1.0; Applied Biosystems), and expression levels for LPL, FATP, and acyl-CoA oxidase were normalized to the 18S rRNA levels.

In vitro PPAR activation assay

HEK293 cells were grown in DMEM plus 10% FCS. Cells were seeded on 96-well plates the day before transfection to give a confluence of 50–80% at transfection. A total of 0.8 μg of DNA containing 0.64 μg of pM1α/γLBD, 0.1 μg of pCMVβGal, 0.08 μg of pGL2$(Gal4)_5$, and 0.02 μg of pADVANTAGE was transfected per well using FuGene transfection reagent according to the manufacturer's instructions (Roche). Cells were allowed to express protein for 48 h followed by the addition of compound.

Human PPAR-α, -γ, and -δ cDNAs were obtained by PCR amplification using cDNA synthesized by reverse transcription of mRNA from human liver, adipose tissue, and placenta, respectively. Amplified cDNAs were cloned into pCR2.1 and sequenced. The ligand binding domain (LBD) of each PPAR isoform was generated by PCR (PPAR-α, amino acid 167 to the C terminus; PPAR-γ, amino acid 165 to the C terminus; PPAR-δ, amino acid 128 to the C terminus) and fused to the DNA binding domain of the yeast transcription factor GAL4 by subcloning fragments in frame into the vector pM1 (13), generating the plasmids pM1αLBD, pM1γLBD, and pM1δLBD. Ensuing fusions were verified by sequencing. The reporter was constructed by inserting an oligonucleotide encoding five repeats of the GAL4 recognition sequence [5× CGGAGTACTGTCCTCCG(AG)] (14) into the vector pGL2 promotor (Promega, Madison, WI), generating the plasmid pGL2$(GAL4)_5$. pCMVβ-Gal was purchased from Clontech, and pADVANTAGE was purchased from Promega.

All PPAR-α ligands were dissolved in DMSO and diluted 1:1,000 upon addition to the cells. Compounds were tested in quadruple in concentrations ranging from 0.001 to 300 μM. Cells were treated with compound for 24 h followed by luciferase assay. Each compound was tested in at least three separate experiments.

Medium including test compound was aspirated, and 100 μl of PBS including 1 mM Mg^{2+} and Ca^{2+} was added to each well. The luciferase assay was performed using the LucLite kit according to the manufacturer's instructions (Packard Instruments). Light emission was quantified by counting on a Packard LumiCounter. To measure β-galactosidase activity, a 25 μl supernatant from each transfection lysate was transferred to a new microplate. β-Galactosidase assays were performed on the microwell plates using a kit from Promega and read in a Labsystems Ascent Multiscan reader. The β-galactosidase data were used to normalize transfection efficiency and cell growth for the luciferase data.

The activity of a compound is calculated as fold induction compared with an untreated sample. For each compound, the efficacy (maximal activity) is given as relative activity compared with Wy-14643 for PPAR-α, rosiglitazone for PPAR-γ, and carbacyclin for PPAR-δ. The EC_{50} is the concentration giving 50% of maximal observed activity. EC_{50} values were calculated via nonlinear regression using GraphPad PRISM 3.02 (GraphPad Software, San Diego, CA). The results are expressed as means ± SD.

PPAR activation in vivo

Male Sprague Dawley rats (Crl:CD BR; Charles River, Sulzfeld, Germany), 6 weeks of age, 280 g body weight, were fed a HCD (1.25% cholesterol; C 13002; Research Diets, Inc.) for 10 days. The cholesterol feeding induced a severe hypercholesterolemia and modest hypertriglyceridemia, whereas serum glucose and insulin remained within the range of normal chow-fed rats. Upon 6 days of feeding, HCD animals were administrated vehicle (1 ml/kg), NNC 61-3058 (10 mg/kg), NNC 61-4424 (10 mg/kg), NNC 61-4706 (10 mg/kg), NNC 61-4718 (10 mg/kg), fenofibrate (300 mg/kg), rosiglitazone (30 mg/kg), or Wy-14643 (10 mg/kg) orally daily for the subsequent 4 days. These doses have previously been determined to induce maximal efficacy in our laboratory. A group of rats fed normal chow was included in parallel. A total of six animals were allocated per group. Nonfasted blood samples were collected from the retro-orbital sinus into plain tubes. Total serum cholesterol, circulating concentrations of HDL-cholesterol, and serum triglycerides were measured after 4 days of treatment on the last day on HCD. Liver weight was measured at the end of the study. Body weight and 24 h food intake were measured on day 10. All serum analyses were performed on a Hitachi 912 autoanalyzer (Roche). Data are presented as means with variations of the mean. Fenofibrate and carbacyclin was purchased from Sigma, and Wy-14643 (C1323) was purchased from Tokyo Kasai Kogyo Co., Ltd. (Toshima, Tokyo, Japan). The compounds rosiglitazone (15), NNC 61-4424 (16), NNC 61-3058 (17), NNC 61-4706 (18), and NNC 61-4718 (17) were all synthesized according to published procedures.

Partial least-squares projection to latent structures analysis

The partial least-squares projection to latent structures (PLS) analysis was performed with Simca-P 9 software (Umetrics, Umea, Sweden). The normalized signal intensities from the 19 genes listed in Table 2 in both color combinations (Cy-3 and Cy-5) were used as single observations (predictor variables). All variables were centered and scaled to unit variance, and log transformed, before the PLS analysis was performed.

RESULTS

In vitro PPAR activation

In vitro receptor transactivation assays with the binding domains of each of the three PPAR receptor subtypes were used to determine the profile of PPAR activation capacity of both the standard and the test compounds. To compare the efficacy of compounds between tests, Wy-14643, rosiglitazone, and carbacyclin were used as reference agonists in the PPAR-α, PPAR-γ, and PPAR-δ transactivation assays, respectively. Maximum obtained fold activation with the reference agonist (~20-fold with Wy-14643 in the PPAR-α assay, 120-fold with rosiglitazone in the PPAR-γ assay, and 250-fold with carbacyclin in the PPAR-δ assay) was defined as 100%. The in vitro PPAR-activating properties of the compounds used in this study are listed in **Table 1**.

As is evident from Table 1, the compounds were selected to display varying PPAR-α efficacies. The efficacious PPAR-γ activator rosiglitazone was included as a reference compound displaying low PPAR-α efficacy. The structures of the selected compounds are shown in **Fig. 1**.

In vivo pharmacological characterization

As a model for diet-induced dyslipidemia, Sprague Dawley rats were fed a HCD containing 1.25% cholesterol, 0.5% cholic acid, and 15% fat (12) for 6 days before drug administration. The diet-induced changes in plasma triglyceride [1.25 ± 0.16 nmol/l (normal chow) → 2.03 ± 0.53 nmol/l (HCD)], total cholesterol [1.79 ± 0.26 nmol/l (normal chow) → 11.98 ± 3.20 nmol/l (HCD)], and HDL-cholesterol [1.15 ± 0.18 nmol/l (normal chow) → 0.84 ± 0.54 nmol/l (HCD)] in animals treated with vehicle are shown in **Fig. 2**. The compounds listed in Table 1 were subsequently administered orally once per day to the animals for 4 days.

Compounds were given at doses previously determined to induce maximal efficacy for the pharmacodynamic parameters of interest (data not shown). The levels of plasma triglyceride, total cholesterol, and HDL-cholesterol were measured on the last day of treatment. The induced changes are shown in **Fig. 3**. All compounds caused a decrease of plasma triglyceride and total cholesterol. The reduction of plasma triglycerides ranged from 11% (rosiglitazone) to 74% (NNC 61-4424). The most pro-

TABLE 1. PPAR-activating characteristics of eight different compounds

Compound	PPAR-α	PPAR-γ	PPAR-δ	PPAR-α EC_{50}	PPAR-γ EC_{50}	PPAR-δ EC_{50}
		% max			*μM*	
Fenofibrate	265 ± 34	8 ± 3	1 ± 0	32.1 ± 9.5	n.d.	n.d.
NNC 61-3058	165 ± 58	128 ± 7	268 ± 18	0.6 ± 0.3	2.9 ± 1.7	10.1 ± 0.1
NNC 61-4424	140 ± 12	108 ± 18	3 ± 0	0.4 ± 0.2	0.2 ± 0.1	n.d.
NNC 61-4718	122 ± 27	99 ± 8	126 ± 24	0.3 ± 0.1	0.1 ± 0	9.3 ± 2.0
NNC 61-4706	137 ± 20	100 ± 21	110 ± 34	0.1 ± 0	0.2 ± 0.1	3.1 ± 0.5
Wy-14643	100	30 ± 4	6 ± 6	12.6 ± 1.1	22.0 ± 2.8	n.d.
Rosiglitazone	43 ± 8	100	7 ± 5	4.1 ± 1.4	0.2 ± 0	n.d.
Carbacyclin	79 ± 35	24.2 ± 6	100	1.1 ± 0.7	7.9 ± 3.1	2.12 ± 0.8

Relative efficacies are calculated as maximal activities relative to Wy-14643 for peroxisome proliferator-activated receptor-α (PPAR-α), rosiglitazone for PPAR-γ, and carbacyclin for PPAR-δ. EC_{50}, concentration giving 50% of maximal observed activity; n.d., not determinable.

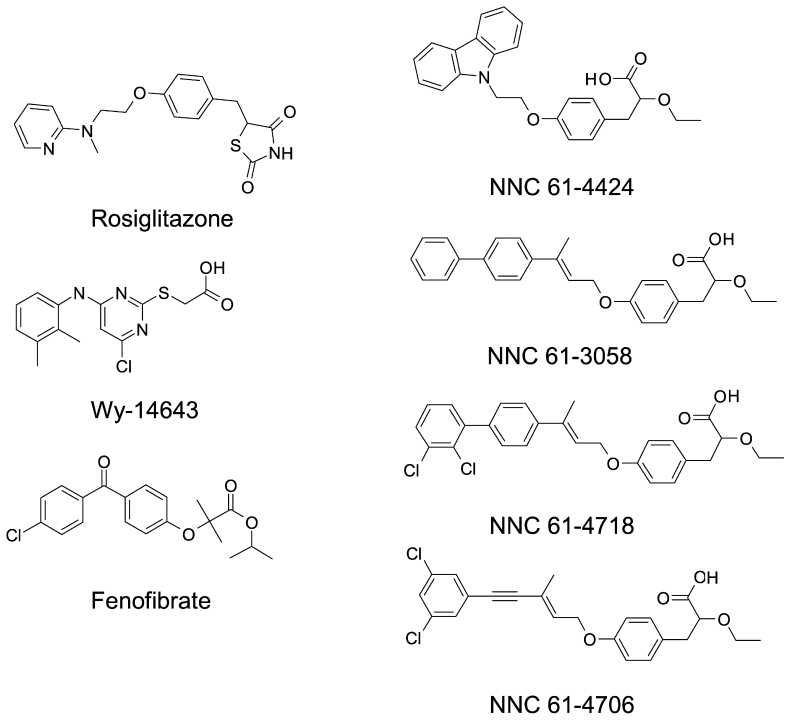

Fig. 1. Chemical structures of the tested compounds: rosiglitazone, Wy-14643, fenofibrate, NNC 61-4424, NNC 61-3058, NNC 61-4718, and NNC 61-4706.

nounced decrease of plasma total cholesterol was observed with fenofibrate (71% reduction). HDL levels were increased by Wy-14643 (18%), rosiglitazone (62%), NNC 61-3058 (100%), and fenofibrate (302%), whereas marginal reductions were observed for the rest of the compounds. Because PPAR-α agonists are known to cause peroxisomal proliferation in livers of rodents, increases in liver weights were also measured from all treatment groups. Normalized liver weights (liver weights as percentage of total body weights) increased the most with dosing of fenofibrate [5.8 ± 0.3 → 8.0 ± 0.3 (+37.9%)] and Wy-14643 [5.6 ± 0.4 → 6.9 ± 0.4 (+23.2%)], but significant increases were also observed for NNC 61-3058 [5.6 ± 0.4 → 6.7 ± 0.3 (+19.6%)], NNC 61-4706 [5.6 ± 0.4 → 6.4 ± 0.4 (+14.3%)], and NNC 61-4718 [5.6 ± 0.4 → 6.2 ± 0.2 (+10.7%)]. Treatment groups dosed with rosiglitazone [5.8 ± 0.3 → 5.7 ± 0.3 (−1.7%)] and NNC 61-4424 [5.7 ± 0.2 → 5.9 ± 0.4 (+3.5%)] did not exhibit any significant change in liver weights.

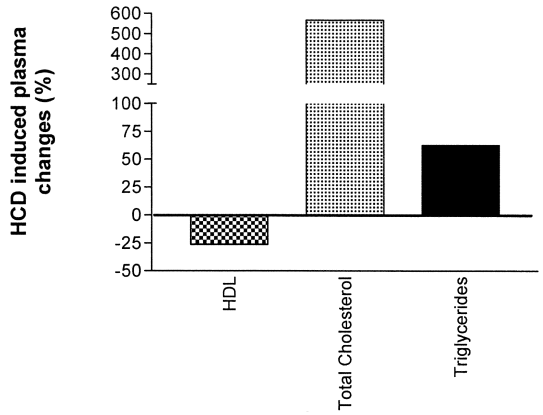

Fig. 2. High-cholesterol diet (HCD) effects on plasma lipid parameters. Percentage changes in plasma lipid parameters (HCD-fed rats relative to chow-fed controls).

cDNA microarray analyses

To gain insight into the underlying patterns of transcriptional changes induced by the PPAR agonists, cDNA microarray analyses were performed on RNA extracts from liver. Total RNA was prepared from individual animals, and pools were generated from each of the animal groups (n = 6). A cDNA microarray containing 2,400 murine genes was used. This gene collection included 132 PPAR-regulated clones previously identified by differential display (19) along with 20 previously identified PPAR-α targets. Furthermore, 125 clones encoding enzymes of the major carbohydrate- and lipid-metabolizing biochemical pathways and 125 transcription factors were included in the array. Finally, ∼2,000 nonredundant randomly selected clones constituted the remainder of this gene collection. All experiments were performed as dual-color hybridizations using the Cy-3 and Cy-5 fluorescent dyes to label the reference and test samples, respectively. Experiments were repeated with reversed dyes in the labeling of test and reference RNA. A total of 89 genes were found to be regulated by at least one of the compounds when accepting only clones that were found to be at least 2-fold regulated and consistently regulated irrespective of dye combination. To focus on the transcriptional changes that were most likely to be a direct consequence of the PPAR-α stimulation, genes that were 2-fold or higher regulated by at least three compounds were identified and are listed in **Table 2**.

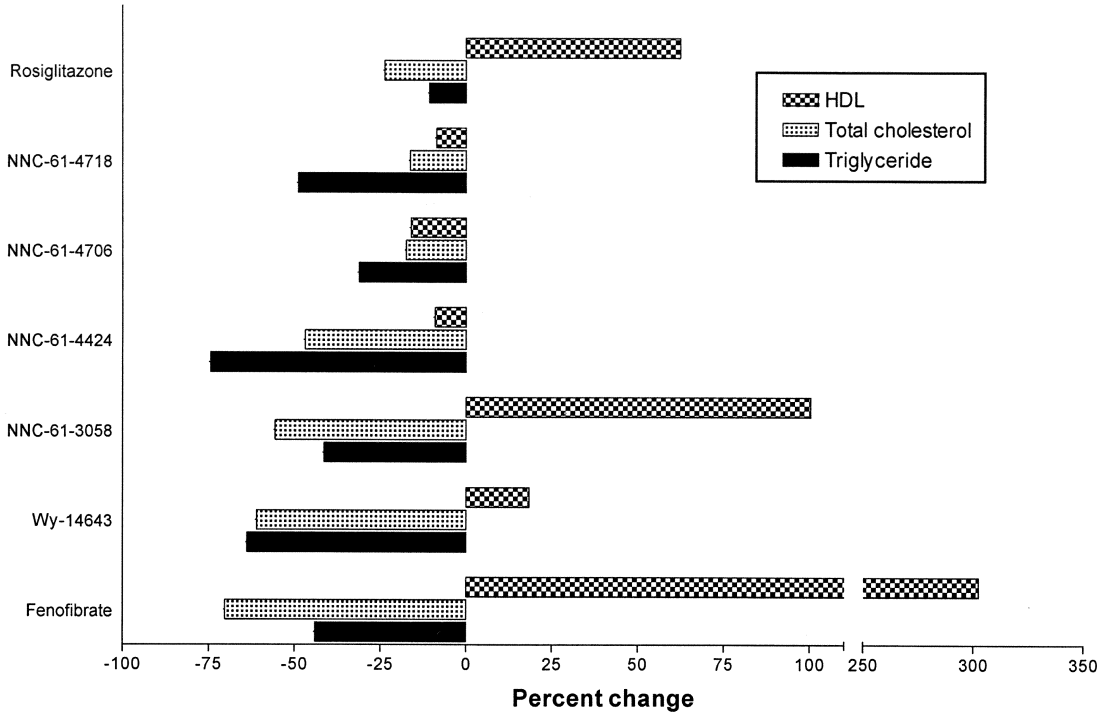

Fig. 3. Pharmacodynamics of the tested compounds. Changes in plasma lipid parameters in Sprague Dawley rats fed a HCD after 4 days of oral treatment. All changes are relative to vehicle-treated rats fed a HCD.

Identification of biomarker genes

To investigate whether the quantitative regulation of the genes listed in Table 2 reflected the in vitro efficacies of the drugs, the fold change of each gene was plotted as a function of the relative efficacy. For the genes encoding peroxisomal bifunctional enzyme, cytochrome P450 4A10 (Cyp4A10), diazepam binding inhibitor [acyl-CoA binding protein (ACBP)], and apoC-III, very good linear correlations between the expression changes and the relative in vitro efficacies of the ligands were found. Linear regression coefficients for these four genes are 0.8 or greater. To confirm the findings of the microarray experiments and the correlation to the in vitro efficacies, Northern blot analysis were done on these regulated genes. The Northern blot data for apoC-III and bifunctional enzyme confirmed the microarray data and the correlations to the relative in vitro efficacies (**Fig. 4**). Cyp4A10 and ACBP were also clearly shown to be regulated based on the Northern blot data, but the correlation to relative efficacies was weaker (r^2 values between 0.5 and 0.6) than the correlation found based on the microarray data. Intensities from the Northern blots were normalized to the signal intensities for ribosomal phosphoprotein 36B4, which has previously been shown not to be regulated by PPAR-α agonists in rat liver (6).

In the hope of identifying biomarker genes whose expression correlate to one or more of the physiological parameters, each gene of the identified gene set was tested for such behavior. Whereas none of the identified regulated genes on their own correlates very well to the changes in either total cholesterol or triglycerides, apoC-III reduction was found to correlate inversely to the increase in HDL levels (**Fig. 5**). It is noteworthy that the outlier in Fig. 5 is rosiglitazone, which does not significantly regulate any of the PPAR-α target genes (Table 2). The increases in liver weights of the different treatment groups correlated to neither any of the physiological parameters nor to the relative in vitro efficacies of the PPAR-α agonists.

Even though apoC-III appears to be a useful biomarker for HDL increase and the relative in vitro PPAR-α efficacy also to a certain, but lesser, degree correlates to this pharmacodynamic property (Fig. 4A), the PPAR-α efficacies found in vitro fail to describe the physiological changes very well. More complex information, such as the combined expression profiles from multiple genes, may be a better way of predicting physiological outcomes based on gene expression changes.

In an attempt to describe the observed pharmacodynamic changes as observed in vivo (Fig. 3) by using all of the found transcriptional changes, multivariate data analysis was invoked. PLS uses a linear multivariate model to relate two data matrices (X) and (Y) (20). Using PLS analysis, all of the regulated gene expression changes (Table 2) were defined as predictor variables (X) and the pharmacological parameters were defined as dependent variables (Y). PLS, unlike multiple linear regression, can analyze highly correlated X variables. Here, rather than using ratios, the normalized signal intensities for the given genes from treated and control animals in both color

TABLE 2. Genes identified to be significantly regulated in common by several compounds

GenBank Accession No.	Gene Name	Fold Regulations: Fenofibrate	Wy-14643	NNC 61-3058	NNC 61-4424	NNC 61-4706	NNC 61-4718	Rosiglitazone
K03249	Peroxisomal enoyl-CoA: hydrotase-3-hydroxyacyl-CoA bifunctional enzyme	38.4	(7.3) 10.4	13.7	9.2	(7.4) 10.6	6.2	1.4
AB018421	Cytochrome P450 4A10	38.2	(9.6) 13.8	13.4	15.8	(8.0) 11.5	10.6	1.5
m26756	Malic enzyme mRNA	31.1	(4.3) 3.7	2.8	1.6	(1.9) 2.4	1.8	1.5
aa870693	L-Lactate dehydrogenase (M-chain)	8.8	(4.2) 5.9	3.9	6.2	(3.4) 3.7	3.0	3.7
aa674347	Acetyl-CoA C-acyltransferase, β-ketothiolase	7.7	(1.4) 2.2	2.3	2.1	(1.5) 2.4	1.7	1.1
aa717130	Acetyl-CoA C-acetyltransferase	6.4	(4.4) 6.5	4.5	3.7	(2.9) 4.5	4.1	1.2
X61431	mRNA for diazepam binding inhibitor (acyl-CoA binding protein)	5.5	(5.2) 2.6	3.1	2.0	(2.1) 2.3	2.2	0.8
U15977	Long-chain fatty acyl CoA synthetase	4.6	(1.4) 3.4	4.7	2.4	(1.9) 2.5	2.3	1.2
L13619	Growth response protein (CL-6) mRNA	4.6	(0.6) 0.4	2.0	0.4	(0.8) 2.1	1.2	3.2
X61147	*Mus musculus* mRNA for iron-responsive element binding protein	3.0	(1.5) 3.0	1.8	1.2	(1.2) 2.1	1.6	1.0
BC003278	EST, similar to ubiquitin-specific protease	3.0	(2.3) 1.4	1.0	0.4	(0.7) 1.2	1.2	0.5
AF144101	Succinyl-CoA synthetase (Sucla1) mRNA	2.7	(2.0) 2.3	2.7	1.4	(1.6) 2.4	2.0	0.9
AA797169	Long-chain acyl-CoA dehydrogenase	2.5	(2.0) 2.6	2.6	3.2	(1.5) 2.1	1.9	1.2
U12791	HMG-CoA synthase	1.9	(1.3) 4.1	3.4	1.1	(6.6) 2.6	2.3	1.0
AB017130	Hex(prh) gene, exon 1	0.5	(1.0) 0.5	0.8	0.6	(0.5) 0.6	0.8	2.9
AI182326	Glucose transporter type 2, liver, GLUT-2	0.4	(0.3) 0.3	0.3	1.1	(0.4) 0.6	0.4	1.2
AA833220	Phosphatidylinositol 3-kinase regulatory γ-subunit	0.4	(0.5) 0.4	0.3	0.5	(0.7) 0.5	0.4	0.7
AA451446	1,4-α-Glucan branching enzyme	0.2	(0.3) 0.4	0.4	0.9	(0.8) 0.7	0.6	0.9
L04150	Apolipoprotein C-III	0.2	(0.6) 0.3	0.2	0.3	(0.6) 0.3	0.4	0.7
J02752[a]	Acyl-CoA oxidase	18.0	10.9	18.1	9.1	5.0	7.9	1.4
L03294[a]	Lipoprotein lipase	10.1	3.25	15.0	5.8	8.4	27.5	1.3
U89529[a]	Fatty acid transport protein	3.0	2.0	4.5	3.2	1.5	2.9	0.8

Hepatic gene expression was analyzed using a cDNA microarray containing 2,400 genes. The table lists the selection of genes that are regulated 2-fold or more by at least three of the PPAR-α agonists. Numbers are fold regulations calculated as expression levels from high-cholesterol diet-fed animals treated with compounds versus expression levels from high-cholesterol diet-fed vehicle-treated animals. Fold changes shown in parentheses (for Wy-14643 and NNC 61-4706) denote data from 10 days of compound dosing; all other regulations derive from animals dosed for 4 days as described in Materials and Methods.

[a] Real time PCR analyses of known PPAR target genes that were either undetectable in the microarray analyses (lipoprotein lipase) or not present on the array (fatty acid transport protein and acyl-CoA oxidase).

combinations (Cy-3 and Cy-5) were used as single observations. All variables were centered and scaled to unit variance and log transformed.

By using PLS modeling, it was possible to build a model to predict the PPAR-α-mediated change in triglyceride with good confidence, and this was the pharmacodynamic property that was predicted the best (**Fig. 6**). When validating the PLS model for triglyceride change by permuting the data, the R^2 value, describing the relation between the observed and predicted variables, decreased from 0.88 to 0.18. This strongly indicates that the model for triglyceride lowering is valid and not overfitted. In contrast, using the same set of gene expression data, it was not possible to generate models that could predict either total cholesterol changes or HDL changes. In the latter case, this was predicted just as well simply by following the expression level of apoC-III.

DISCUSSION

In the present study, Sprague Dawley rats fed a HCD (12) were used as a model for diet-induced dyslipidemia to examine physiological and transcriptional changes during treatment with seven structurally different PPAR-α activators. These included the reference compounds fenofibrate, Wy-14643, and rosiglitazone along with four new compounds, NNC 61-3058, NNC 61-4424, NNC 61-4706, and NNC 61-4718. The structural differences (Fig. 1) were reflected in their relative PPAR-α efficacies (ranging from 50% to 265%), and were as such well suited for a comparative study of PPAR-α-mediated transcriptional and physiological changes. The functional similarity (i.e., PPAR-α activation of the compounds) will help to discriminate core PPAR-α-regulated genes from ligand-specific gene regulations.

All of the studied PPAR-α agonists had expectedly a lowering effect on the plasma levels of triglyceride and total cholesterol (Fig. 3). The reduction in plasma levels of triglyceride ranged from 11% for rosiglitazone to 74% for NNC 61-4424. Lowering of triglycerides is the hallmark of fibrates in both humans and animal models, and drugs such as gemfibrozil (21), ciprofibrate (22), bezafibrate, and fenofibrate (23) have been reported to reduce plasma triglycerides in the range of 40–60% in either normal chow- or cholesterol-fed rats. Total plasma cholesterol is also a parameter that has been observed to be reduced

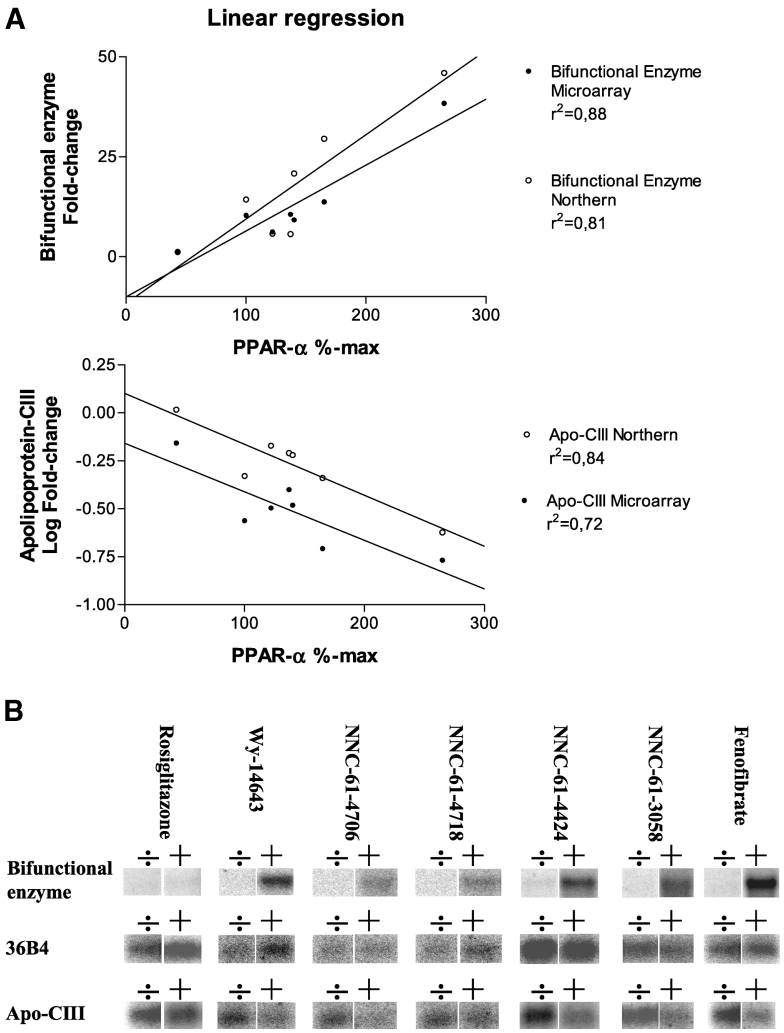

Fig. 4. Relationship between regulated target genes and the relative drug peroxisome proliferator-activated receptor-α (PPAR-α) efficacy. A: Comparison of quantitative expression levels as measured in microarrays and Northern blot analysis and the relative PPAR-α efficacies of the tested compounds using linear regression analysis. Fold regulations as calculated in Table 2 were used for the microarray data, whereas signal intensities for the genes in Northern blots were collected using a PhosphorImager and normalized to the signals for ribosomal phosphoprotein 36B4. For apolipoprotein C-III (apoC-III), the log fold change was used because this gene is downregulated and its expression ratios lie between 1 and 0. B: Northern blots showing the expression of peroxisomal enoyl-CoA:hydrotase-3-hydroxyacyl-CoA bifunctional enzyme (bifunctional enzyme), apoC-III, and ribosomal phosphoprotein 36B4.

by fibrates in rats (24). In the present study, rather large reductions in plasma total cholesterol were observed, with Wy-14653 (60% reduction) and fenofibrate (71% reduction) as the most efficacious drugs. These sizable reductions can most likely be explained by the very large diet-induced increase in total cholesterol. The drug-induced increase in HDL-cholesterol is also very diet-dependent in rats. In chow-fed rats, drugs such as bezafibrate, clofibrate, fenofibrate, and gemfibrozil have shown no HDL-increasing effect (25). But in rats fed a HCD, fenofibrate, ciprofibrate, and especially gemfibrozil have been shown to increase HDL-cholesterol (26, 27). In the present study, an increase in HDL-cholesterol was observed for fenofibrate, NNC 61-3058, and Wy-14653. Surprisingly, an increase in HDL-cholesterol (62%) was also observed for rosiglitazone. For rosiglitazone, this effect seems to be related to other factors than activation of PPAR-α, because NNC 61-4706, NNC 61-4718, and NNC 61-4424, which are more efficacious PPAR-α activators, do not increase HDL but actually marginally reduce HDL in the range of 9–16%. The rosiglitazone-mediated upregulation of HDL levels, however, does raise the question of whether the HDL upregulation mediated by the PPAR-α agonists is an effect solely mediated through PPAR-α activation.

Many of the genes that were found to be regulated (Table 2) are involved in lipid metabolism and have previously been shown to be regulated by PPAR agonists. These include bifunctional enzyme (peroxisomal β-oxidation) (28), Cyp4A10 (microsomal ω-hydroxylation) (29), acetyl-CoA C-acetyltransferase (mitochondrial β-oxidation) (30), β-ketothiolase (mitochondrial β-oxidation), long-chain acyl-CoA dehydrogenase (mitochondrial β-oxidation) (31), long-chain fatty acyl-CoA synthetase (fatty acid activation) (32), ACBP (fatty acid compartmentalization) (33), apoC-III (lipoprotein metabolism) (11), HMG-CoA synthase (ketone body synthesis) (34), and malic enzyme (NADPH supply for fatty acid synthesis) (35). It has also previously been shown that the liver GLUT-2 promotor contains a functional PPAR response element (36). In experiments in which animals were dosed for 10 days with Wy-14643 and NNC 61-4706 (Table 2), gene regulations were found to be very similar to those observed in animals dosed for 4 days. Data indicate a slight tendency toward larger gene expression changes after 4 days of dosing for a number of genes, which might reflect minor transcriptional feedback regulation during longer treatment protocols. In addition to the compound-mediated transcriptional effects, the HCD used may also have influenced the expression pro-

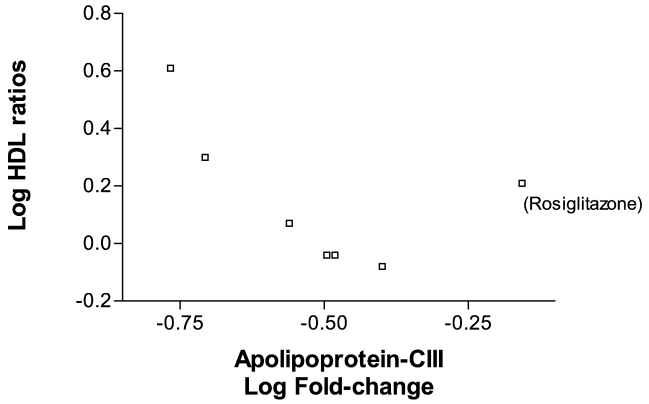

Fig. 5. Relationship between the degree of downregulation observed for apoC-III and the change in HDL-cholesterol. Fold changes for apoC-III were calculated as described in Table 2. Because apoC-III is downregulated (i.e., fold regulations are in the interval between 1 and 0), these values were plotted as log-transformed to expand the scale. HDL ratios were calculated as the HDL levels observed in treated animals (HCD-fed) versus those observed in vehicle-treated animals (HCD-fed).

files of a number of the genes listed in Table 2. Recently, a microarray study of the transcriptional responses to a HCD reported 69 genes as regulated in livers of mice (37). Genes significantly downregulated by the cholesterol component of the diet included malic enzyme, ACBP, and HMG-CoA synthase. These were also regulated in the present study (Table 2) and are as described above known PPAR target genes. Thus, the regulation of these genes was most likely affected by both the ligand-mediated decrease of total cholesterol (Fig. 3) and the direct PPAR-α-mediated transcriptional activation. This emphasizes the importance of the choice of diet for gene expression studies and suggests that predictive gene sets may be most accurate when used in animal models similar to the one in which they were identified.

When searching for possible correlations between the observed in vitro PPAR-α efficacies for each compound and the expression profiles of the regulated genes, a number of very clear relationships were identified (Fig. 4A). The best linear regressions, based on data from both Northern blotting and microarrays, were found for apoC-III and bifunctional enzyme. This is to our knowledge the first time that a relationship between the gene expression profiles from a series of different drug treatments and the efficacy of the included compounds has been reported. These genes may be useful in the in vivo evaluation of new PPAR-α-activating compounds.

Even though expression profiles of single genes can correlate to different pharmacodynamic properties (Fig. 5), models that take multiple variables (e.g., gene expression profiles) into account may provide a much more robust prediction of the physiological response of interest. This may especially be the case for drugs with multiple target points, such as fibrates and thiazolidinediones. Therefore, we used a multivariate model called PLS and defined the expression profiles of the regulated genes (Table 2) as predictor (X) variables and the pharmacodynamic parameters as dependent (Y) variables. The pharmacodynamic property, which was best predicted using the hybridization signals from the regulated genes, was triglyceride lowering (Fig. 6). When plotting the observed triglyceride lowering against the values predicted by the PLS model, a very good correlation was observed (R^2 = 0.88). A very large fraction of the genes used as predictor variables do indeed encode enzymes involved in triglyceride metabolism. In comparison to the very good prediction of triglyceride change, the prediction of the total cholesterol and the HDL level changes were weaker. When plotting the predicted values against the observed values for these parameters, the R^2 values were ~0.6 for the change in plasma total cholesterol and 0.2 for the change in HDL levels. It is very important not to "overfit" PLS models, and any model must always be validated, for example, by permuting the data that should cause an observed correlation between predicted and observed variables to disappear.

In the present study, seven different PPAR-α activators with varying efficacies were dosed in rats fed a HCD. Our

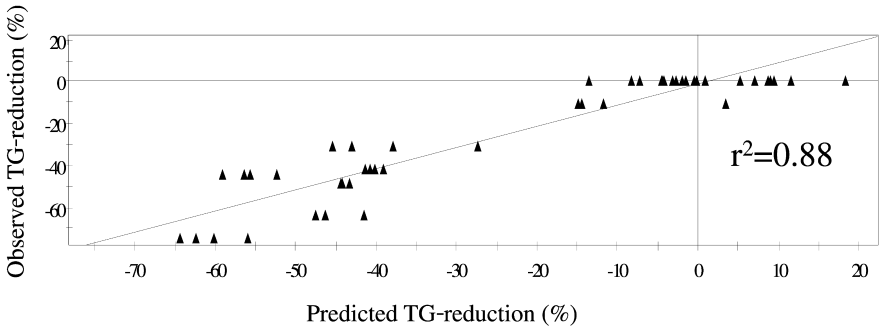

Fig. 6. Generation of a model to predict triglyceride (TG) changes from multivariate gene expression data. Partial least-squares projection to latent structures regression analysis of the change in triglyceride used the observed transcriptional changes listed in Table 2. The four data points shown for each compound represent the normalized signal intensities from the Cy-3- and Cy-5-labeled probe preparations. On the *x* axis, the values for the predicted triglyceride reduction based on gene expression data are plotted. On the *y* axis, the actual data for the triglyceride reduction are plotted.

observations have shown that comparative gene expression profiling in vivo can reveal useful biomarkers that correlate very well to both the receptor-activating properties of the drugs found in vitro and the pharmacodynamic properties observed in vivo. For the prediction of pharmacodynamic parameters, the use of multivariate models such as PLS seems to be a very useful way of interpreting complex gene expression data in a physiological context. Using the information from 19 regulated genes, a very good prediction of the triglyceride-lowering effect of the included drugs could be made. The data from the present study will be useful when evaluating the potential of new PPAR-α activators in rats and demonstrate the applicability of gene expression profiling in the characterization of potentially new drug candidates.

The authors thank Lene Hansen, Tine Pedersen, Anette Seneca, and Rikke Burgdorf for expert technical assistance, Dr. Vladka Panajotova for performing the animal studies, and Drs. Esper Boel and Johan Selmer for critical comments and review of the manuscript.

REFERENCES

1. Issemann, I., and S. Green. 1990. Activation of a member of the steroid hormone receptor superfamily by peroxisome proliferators. *Nature.* **347:** 645–650.
2. Dreyer, C., G. Krey, H. Keller, F. Givel, G. Helftenbein, and W. Wahli. 1992. Control of the peroxisomal beta-oxidation pathway by a novel family of nuclear hormone receptors. *Cell.* **68:** 879–887.
3. Tugwood, J. D., I. Issemann, R. G. Anderson, K. R. Bundell, W. L. McPheat, and S. Green. 1992. The mouse peroxisome proliferator activated receptor recognizes a response element in the 5′ flanking sequence of the rat acyl CoA oxidase gene. *EMBO J.* **11:** 433–439.
4. Gulick, T., S. Cresci, T. Caira, D. D. Moore, and D. P. Kelly. 1994. The peroxisome proliferator-activated receptor regulates mitochondrial fatty acid oxidative enzyme gene expression. *Proc. Natl. Acad. Sci. USA.* **91:** 11012–11016.
5. Muerhoff, A. S., K. J. Griffin, and E. F. Johnson. 1992. The peroxisome proliferator-activated receptor mediates the induction of CYP4A6, a cytochrome P450 fatty acid omega-hydroxylase, by clofibric acid. *J. Biol. Chem.* **267:** 19051–19053.
6. Martin, G., K. Schoonjans, A. M. Lefebvre, B. Staels, and J. Auwerx. 1997. Coordinate regulation of the expression of the fatty acid transport protein and acyl-CoA synthetase genes by PPARalpha and PPARgamma activators. *J. Biol. Chem.* **272:** 28210–28217.
7. Schoonjans, K., J. Peinado-Onsurbe, A. M. Lefebvre, R. A. Heyman, M. Briggs, S. Deeb, B. Staels, and J. Auwerx. 1996. PPAR alpha and PPAR activators direct a distinct tissue-specific transcriptional response via a PPRE in the lipoprotein lipase gene. *EMBO J.* **15:** 5336–5348.
8. Vu, D. N., K. Schoonjans, B. Laine, J. C. Fruchart, J. Auwerx, and B. Staels. 1994. Negative regulation of the human apolipoprotein A-I promoter by fibrates can be attenuated by the interaction of the peroxisome proliferator-activated receptor with its response element. *J. Biol. Chem.* **269:** 31012–31018.
9. Vu, D. N., K. Schoonjans, V. Kosykh, J. Dallongeville, J. C. Fruchart, B. Staels, and J. Auwerx. 1995. Fibrates increase human apolipoprotein A-II expression through activation of the peroxisome proliferator-activated receptor. *J. Clin. Invest.* **96:** 741–750.
10. Chinetti, G., S. Lestavel, V. Bocher, A. T. Remaley, B. Neve, I. P. Torra, E. Teissier, A. Minnich, M. Jaye, N. Duverger, H. B. Brewer, J. C. Fruchart, V. Clavey, and B. Staels. 2001. PPAR-alpha and PPAR-gamma activators induce cholesterol removal from human macrophage foam cells through stimulation of the ABCA1 pathway. *Nat. Med.* **7:** 53–58.
11. Staels, B., D. N. Vu, V. A. Kosykh, R. Saladin, J. C. Fruchart, J. Dallongeville, and J. Auwerx. 1995. Fibrates downregulate apolipoprotein C-III expression independent of induction of peroxisomal acyl coenzyme A oxidase. A potential mechanism for the hypolipidemic action of fibrates. *J. Clin. Invest.* **95:** 705–712.
12. Paigen, B., A. Morrow, C. Brandon, D. Mitchell, and P. Holmes. 1985. Variation in susceptibility to atherosclerosis among inbred strains of mice. *Atherosclerosis.* **57:** 65–74.
13. Sadowski, I., B. Bell, P. Broad, and M. Hollis. 1992. GAL4 fusion vectors for expression in yeast or mammalian cells. *Gene.* **118:** 137–141.
14. Webster, T. D., and R. C. Dickson. 1988. Nucleotide sequence of the galactose gene cluster of Kluyveromyces lactis. *Nucleic Acids Res.* **16:** 8192–8194.
15. Cantello, B. C. C., M. A. Cawthorne, D. Haigh, R. M. Hindley, S. A. Smith, and P. L. Thurlby. 1994. The synthesis of brl-49653—a novel and potent antihyperglycemic agent. *Bioorg. Med.* **4:** 1181–1184.
16. Sauerberg, P., I. Pettersson, L. Jeppesen, P. S. Bury, J. P. Mogensen, K. Wassermann, C. L. Brand, J. Sturis, H. F. Woldike, J. Fleckner, A. S. T. Andersen, S. B. Mortensen, L. A. Svensson, H. B. Rasmussen, S. V. Lehmann, Z. Polivka, K. Sindelar, V. Panajotova, L. Ynddal, and E. M. Wulff. 2002. Novel tricyclic-alpha-alkyloxyphenylpropionic acids: dual PPAR alpha/gamma agonists with hypolipidemic and antidiabetic activity. *J. Med. Chem.* **45:** 789–804.
17. Mogensen, J. P., P. Sauerberg, P. S. Bury, L. Jeppesen, and I. Pettersson. 2001. Propionic acid derivatives and their use in the treatment of diabetes and obesity. US patent WO 01/55085 A1.
18. Mogensen, J. P., P. Sauerberg, P. S. Bury, L. Jeppesen, and I. Pettersson. 2001. Alkynylsubstituted propionic acid derivatives and their use against diabetes and obesity. US patent WO 01/55086 A1.
19. Albrektsen, T., K. S. Frederiksen, W. E. Holmes, E. Boel, K. Taylor, and J. Fleckner. 2002. Novel genes regulated by the insulin sensitizer rosiglitazone during adipocyte differentiation. *Diabetes.* **51:** 1042–1051.
20. Wold, S., M. Sjoström, and L. Eriksson. 2001. PLS-regression: a basic tool of chemometrics. *Chemometr. Intell. Lab. Syst.* **58:** 109–130.
21. Krause, B. R., R. Bousley, K. Kieft, D. Robertson, R. Stanfield, E. Urda, and R. S. Newton. 1994. Comparison of lifibrol to other lipid-regulating agents in experimental animals. *Pharmacol. Res.* **29:** 345–357.
22. Cignarella, A., M. Nastasi, E. Cavalli, and L. Puglisi. 1996. Novel lipid-lowering properties of Vaccinium myrtillus L. leaves, a traditional antidiabetic treatment, in several models of rat dyslipidemia: a comparison with ciprofibrate. *Thromb. Res.* **84:** 311–322.
23. Naderali, E. K., L. C. Pickavance, J. P. H. Wilding, P. J. Doyle, and G. Williams. 2001. Troglitazone corrects metabolic changes but not vascular dysfunction in dietary-obese rats. *Eur. J. Pharmacol.* **416:** 133–139.
24. Krause, B. R., and H. M. G. Princen. 1998. Lack of predictability of classical animal models for hypolipidemic activity: a good time for mice? *Atherosclerosis.* **140:** 15–24.
25. Haubenwallner, S., A. D. Essenburg, B. C. Barnett, M. E. Pape, R. B. DeMattos, B. R. Krause, L. L. Minton, B. J. Auerbach, R. S. Newton, T. Leff, and C. L. Bisgaier. 1995. Hypolipidemic activity of select fibrates correlates to changes in hepatic apolipoprotein C-III expression: a potential physiologic basis for their mode of action. *J. Lipid Res.* **36:** 2541–2551.
26. Krause, B. R., and R. S. Newton. 1986. Gemfibrozil increases both apo A-I and apo E concentrations. Comparison to other lipid regulators in cholesterol-fed rats. *Atherosclerosis.* **59:** 95–98.
27. Petit, D., M. T. Bonnefis, C. Rey, and R. Infante. 1988. Effects of ciprofibrate and fenofibrate on liver lipids and lipoprotein synthesis in normo- and hyperlipidemic rats. *Atherosclerosis.* **74:** 215–225.
28. Bardot, O., T. C. Aldridge, N. Latruffe, and S. Green. 1993. PPAR-RXR heterodimer activates a peroxisome proliferator response element upstream of the bifunctional enzyme gene. *Biochem. Biophys. Res. Commun.* **192:** 37–45.
29. Bell, D. R., N. J. Plant, C. G. Rider, L. Na, S. Brown, I. Ateitalla, S. K. Acharya, M. H. Davies, E. Elias, and N. A. Jenkins. 1993. Species-specific induction of cytochrome P-450 4A RNAs: PCR cloning of partial guinea-pig, human and mouse CYP4A cDNAs. *Biochem. J.* **294:** 173–180.
30. Gould-Rothberg, B. E., S. S. Sundseth, V. A. DiPippo, P. J. Brown, D. A. Winegar, W. K. Gottshalk, S. G. Shenoy, and J. M. Rothberg. 2001. The characterization of PPAR-alpha ligand drug action in an in vivo model by comprehensive differential gene expression profiling. *Funct. Integr. Genomics.* **1:** 294–304.

31. Ouali, F., F. Djouadi, C. Merlet-Benichou, and J. Bastin. 1998. Dietary lipids regulate beta-oxidation enzyme gene expression in the developing rat kidney. *Am. J. Physiol.* **44:** F777–F784.
32. Schoonjans, K., M. Watanabe, H. Suzuki, A. Mahfoudi, G. Krey, W. Wahli, P. Grimaldi, B. Staels, T. Yamamoto, and J. Auwerx. 1995. Induction of the acyl-coenzyme A synthetase gene by fibrates and fatty acids is mediated by a peroxisome proliferator response element in the C promoter. *J. Biol. Chem.* **270:** 19269–19276.
33. Elholm, M., G. Bjerking, J. Knudsen, K. Kristiansen, and S. Mandrup. 1996. Regulatory elements in the promoter region of the rat gene encoding the acyl-CoA-binding protein. *Gene.* **173:** 233–238.
34. Rodriguez, J. C., G. Gil-Gomez, F. G. Hegardt, and D. Haro. 1994. Peroxisome proliferator-activated receptor mediates induction of the mitochondrial 3-hydroxy-3-methylglutaryl-CoA synthase gene by fatty acids. *J. Biol. Chem.* **269:** 18767–18772.
35. Castelein, H., T. Gulick, P. E. Declercq, G. P. Mannaerts, D. D. Moore, and M. I. Baes. 1994. The peroxisome proliferator activated receptor regulates malic enzyme gene-expression. *J. Biol. Chem.* **269:** 26754–26758.
36. Kim, H., J. Kim, S. Kim, J. Y. Cha, K. S. Kim, and Y. Ahn. 2000. Identification and functional characterization of the peroxisomal proliferator response element in rat GLUT2 promoter. *Diabetes.* **49:** 1517–1524.
37. Maxwell, K. N., R. E. Soccio, E. M. Duncan, E. Sehayek, and J. L. Breslow. 2003. Novel putative SREBP and LXR target genes identified by microarray analysis in liver of cholesterol-fed mice. *J. Lipid Res.* **44:** 2109–2119.

ERRATA

In the article "Substrate reduction reduces gangliosides in postnatal cerebrum-brainstem and cerebellum in GM1 gangliosidosis mice" by Kasperzyk et al., published in the April 2004 issue of the *Journal of Lipid Research* (Volume **46**, pages 744–751), the affiliations should read as follows:

J. L. Kasperzyk,* A. d'Azzo,† F. M. Platt,§ J. Alroy,** and T. N. Seyfried*,[1]

Department of Biology,* Boston College, Chestnut Hill, MA; Department of Genetics,† St. Jude Children's Research Hospital, Memphis, TN; Glycobiology Institute,§ Department of Biochemistry, University of Oxford, Oxford, United Kingdom; and Department of Pathology,** Tufts University School of Medicine and Veterinary Medicine, New England Medical Center, Boston, MA

[1]To whom correspondence should be addressed.
e-mail: thomas.seyfried@bc.edu

*****

In the article "Prediction of PPAR-α ligand-mediated physiological changes using gene expression profiles" by Frederiksen et al., published in the March 2004 issue of the *Journal of Lipid Research* (Volume **45**, pages 592–601), the digital object identifier (DOI) should read: DOI 10.1194/jlr.M300239-JLR200.

*****

In the article "Regulation of ganglioside biosynthesis in the nervous system" by Yu et al., published in the May 2004 issue of the *Journal of Lipid Research* (Volume **45**, pages 783–793), the digital object identifier (DOI) should read: DOI 10.1194/jlr.R300020-JLR200.

*****

In the article "Cholesterol metabolism in the central nervous system during early development and in the mature animal" by Dietschy and Turley, published in the August 2004 issue of the *Journal of Lipid Research* (Volume **45**, pages 1375–1397), the digital object identifier (DOI) should read: DOI 10.1194/jlr.R400004-JLR200.